Energy 183 (2019) 504–513

Contents lists available at ScienceDirect

Energy

journal homepage: www.elsevier.com/locate/energy

Optimization of supercapacitor sizing for high-fluctuating power applications by means of an internal-voltage-based method

Joaquín F. Pedrayes*, Manuel G. Melero, José M. Cano, Joaquín G. Norniella, Gonzalo A. Orcajo, Manés F. Cabanas, Carlos H. Rojas

Departamento de Ingeniería Eléctrica, Electrónica, de Computadores y Sistemas, Universidad de Oviedo, Spain

ARTICLE INFO

Article history:
Received 23 November 2018
Received in revised form
21 May 2019
Accepted 23 June 2019
Available online 26 June 2019

Keywords:
Energy storage
Hybrid systems
Size optimization.
Supercapacitor

ABSTRACT

The latest advances in the field of supercapacitors (SCs) have made them a feasible alternative to be used in hybrid, energy storage systems. Sizing SCs in such systems is not obvious, especially in the case of banks comprising several series-parallel configurations. In this paper, a new algorithm for sizing a SC bank in high fluctuating power demand applications is proposed. The algorithm utilizes the expected discharge power profile, usually obtained from measurement campaigns, and a set of resistance (***R***) and capacitance (***C***) values of the equivalent circuit of the SC, which are provided by the manufacturer. Instead of yielding specific values for ***R*** and ***C***, the method determines the RC limit curve which identifies the area of the RC-plane where the range of acceptable solutions can be found for a particular application. Thus, the internal resistance can be easily included in the design process. The validity of different cell combinations, including those not regarding each series-connected element as a sole cell, can be directly checked with this method, enabling the selection of the most suitable solution from an economic point of view.

© 2019 The Authors. Published by Elsevier Ltd. This is an open access article under the CC BY-NC-ND license (http://creativecommons.org/licenses/by-nc-nd/4.0/).

1. Introduction

Supercapacitors (SCs) are devices able to provide high power for short periods, which make them suitable in applications where it is necessary to supply transient current peaks and to absorb fast fluctuations of energy demand. The latest advances have made them a feasible alternative in a good number of energy storage applications [1]. Specifically, SCs are becoming a crucial part in the development of hybrid energy storage systems (HESSs), where they can be found combined with batteries [2–6], compressed air [7] or fuel cells [8]. In all of these cases, the SC compensates for the transient peaks and rapid load fluctuations, while the main storage device is in charge of average components. HESSs are becoming popular in many applications such as electric vehicles [9–11], but they can also be found in electric grids [8] or, even, in hybrid electric construction machinery [12]. In those systems, the combination of batteries and SCs is specially interesting, since the former are exposed to damage when subjected to sudden changes in their charge/discharge processes. SCs present clear advantages, such as high charge/discharge currents and specific power values, low internal resistances [13,14], and long life expectancy. Indeed, SCs expected charge/discharge cycle life is typically around a million, while batteries can hardly withstand 400-4000 cycles, depending on technology [15]. Thus, the use of a HESS based on a battery-SC configuration can be extremely useful to enlarge the life expectancy of the setup [9].

When it comes to optimizing the capacitance needed for a specific application, some sizing methods calculate the required value by considering the cells as ideal conventional capacitors [16] and regarding only the stored energy. However, as is demonstrated in this proposal, such methods may be not suitable when working with high power values because of the constraint imposed by the internal resistance of the cells.

Regarding SC models that can be found in the literature, some of them are developed to analyze the behavior of the cells when being subjected to currents with high and low-order harmonic components [17] or to a wide range of temperatures. Other models are non-linear [18] or use a variable capacitance dependent on the SC internal voltage [19,20]. The series-RC is the most widely used model for sizing issues, where the utilized capacitance is considered as a constant parameter. The values of both the capacitance and the resistance of the different cells are provided by the

* Corresponding author.
E-mail address: pedrayesjoaquin@uniovi.es (J.F. Pedrayes).

https://doi.org/10.1016/j.energy.2019.06.145
0360-5442/© 2019 The Authors. Published by Elsevier Ltd. This is an open access article under the CC BY-NC-ND license (http://creativecommons.org/licenses/by-nc-nd/4.0/).

manufacturer [21–26]. Some existing models include the parallel resistance to take into account the self-discharge of the cells [27,28], but this feature is normally neglected in the sizing process.

Other sizing methods utilize the so-called "state of charge" [29] or "state of energy" [30]. More specifically, in Ref. [30] a non-iterative sizing strategy where the resulting cells are slightly oversized is used; series-connected components are regarded as just one cell, the possibility for such components to be a combination of different parallel-connected cells being dismissed.

In this paper, a new sizing algorithm based on the calculation of the RC limit curve is proposed. The curve identifies an area comprising infinite theoretical acceptable solutions and is obtained from the worst-case RC values of the cells, i.e. those expected at the end of their service life. The proposed method allows verifying whether different cell combinations are valid for a specific application. Thus, the proposal greatly simplifies the selection of the final solution from an economic point of view. The method regards the possibility for series-connected components to be a combination of various parallel-connected cells, which expands the range of possible solutions and enables the design of the most suitable configuration. Moreover, the method provides the tools to calculate additional parameters of the proposed solution in the context of its particular application, which can be used to check the compliance to particular constraints such as current discharge limits.

The paper is structured as follows: Section 2 describes the use of SCs for compensating the power oscillations of a load, which is usually known in the literature as load leveling or peak shaving. In Section 3, the behavior of a SC connected to a constant-power source is approached. Section 4 introduces the concept of RC limit curve and formulates its calculation, which is exemplified in Section 5 by means of a case study. Section 6 shows a summary of the advantages of this method and finally, the conclusions of this paper are drawn and presented in Section 7.

2. SCs and power oscillations compensation

The use of SCs is particularly interesting when it comes to compensate for load power oscillations. In Fig. 1, an example, usually known as load leveling, is shown. The SC bank aims to smooth the power demand as seen from the grid to the greatest possible extent. The power absorbed by the SC bank, $p(t)$, compensates for the oscillating power, $p_B(t)$, absorbed by the load (system B), its mean value, $p_A(t)$, thus being supplied by the main source (system A),

$$p_A(t) = \text{mean}(p_B(t)) \tag{1}$$

In this case, the calculation of the required capacitance is not straightforward. The SC bank, initially charged with a stand-by voltage, is successively charged and discharged according to the power profile given by $p(t)$. In this process, the internal voltage of the cells must be within the acceptable maximum and minimum limits supplied by the manufacturer. Moreover, the current through the cells must be lower than a specific value to avoid damage due to overheating.

The power profile given by $p_B(t)$ represents the input data of the sizing problem. This profile can be obtained by measuring the power consumption directly, in the case of existing loads, or using simulations or estimated calculations of the process during the design stage. The response of the DC/DC converter is assumed to be much faster than the load power oscillations. Then,

$$p(t) = p_A(t) - p_B(t) = \overline{p_B} - p_B(t), \tag{2}$$

where $\overline{p_B}$ is the average value of. $p_B(t)$.

3. Behavior of SCs at constant power

The SC bank power profile given by $p(t)$. is regarded in this section as a succession of power values that are constant for a specific time interval. Therefore, the SC bank can be assumed to be charging/discharging at constant power during such intervals. Notice that the accuracy of the latter statement will be acceptable provided that the appropriate sampling rate is selected when capturing the dynacs of t power profile. Fig. 2 shows the equivalent resistance, R., and capacitance, C, and the internal, u, and external, u_{co}, voltages of the SC bank when charged at a constant power value, P.

According to the scheme shown in Fig. 2,

$$\boldsymbol{P} - \boldsymbol{R}\cdot\boldsymbol{i}^2 = \boldsymbol{u}\cdot\boldsymbol{i}, \tag{3}$$

$$\frac{du}{dt} = \dot{u} = \frac{i}{C} \tag{4}$$

By combining (3) and (4),

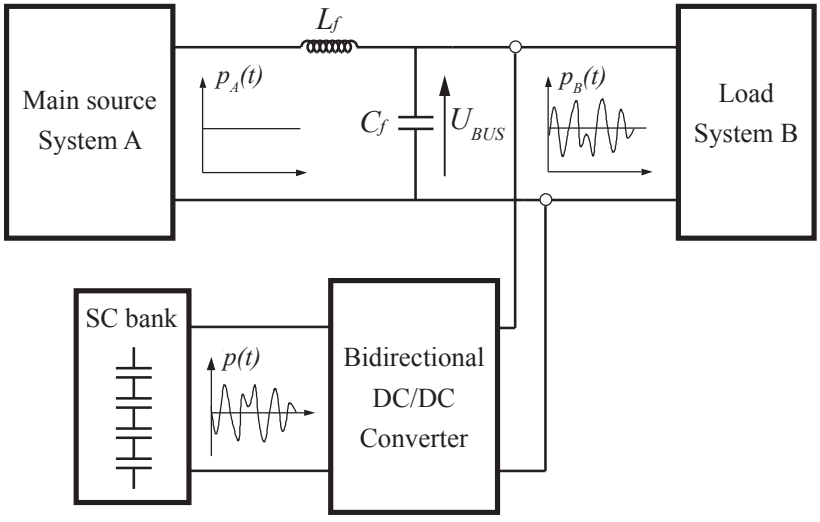

Fig. 1. Use of a SC bank for the compensation of power oscillations.

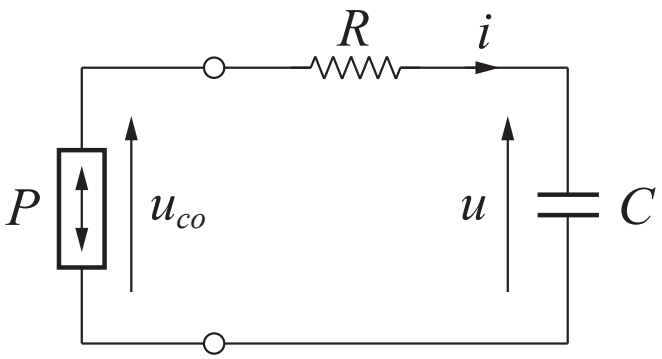

Fig. 2. Charge of a SC at constant power.

$$R \cdot C^2 \cdot \dot{u}^2 + C \cdot u \cdot \dot{u} - P = 0 \tag{5}$$

Dividing (5) over $R \cdot C^2$ yields

$$\dot{u}^2 + \frac{u}{R \cdot C} \cdot \dot{u} - \frac{P}{R \cdot C^2} = 0, \tag{6}$$

where $P > 0$ for a charge and $P < 0$ for a discharge. Solving (6) for $\dot{u}$ yields

$$\dot{u} = \frac{-u}{2 \cdot R \cdot C} + \frac{\sqrt{u^2 + 4 \cdot P \cdot R}}{2 \cdot R \cdot C} \tag{7}$$

In solving (7), the time, t, needed for the internal voltage to change from its previous voltage, u_p, to its final value, given by u, can be obtained, and is shown in (8). That time depends on the power given by P and on the resistance and capacitance parameters of the equivalent cell.

$$t = \frac{C}{4 \cdot P} \cdot \left[u^2 - u_p^2 + u \cdot \sqrt{u^2 + 4 \cdot P \cdot R} - u_p \cdot \sqrt{u_p^2 + 4 \cdot P \cdot R} - 4 \cdot P \cdot R \cdot ln\left(\frac{u_p + \sqrt{u_p^2 + 4 \cdot P \cdot R}}{u + \sqrt{u^2 + 4 \cdot P \cdot R}} \right) \right] \tag{8}$$

As can be deduced, an infinite number of RC combinations meet (8) for specific given values of P and t.

4. RC limit curve: description and calculation

The standard sizing problem regards a SC bank subjected to a succession of charges and discharges. The power profile can be always discretized according to a selected sample time, either fix or variable. Fig. 3 shows an example of a power profile given by $\mathbf{P} = [\mathbf{P_1}, \mathbf{P_2} \ldots, \mathbf{P_n}]$,$\mathbf{t} = [\mathbf{T_1}, \mathbf{T_2} \ldots, \mathbf{T_n}]$.

The maximum and minimum acceptable values of the internal voltage are required to size the SC bank. The maximum internal voltage, $\boldsymbol{U_{MAX}}$, is usually set by the dc-bus voltage, $\boldsymbol{U_{BUS}}$, and determines the number of series-connected components to be used in the bank. As for the minimum internal voltage, $\boldsymbol{U_{MIN}}$, it has to have a value such the voltage of each cell must be no lower than 50% of the rating value, $\boldsymbol{U_{SCN}}$, as recommended by the manufacturer. The typical range of values for $\boldsymbol{U_{SCN}}$ is 2.7–3.0 V. From $\boldsymbol{U_{BUS}}$ and $\boldsymbol{U_{SCN}}$, the number of series-connected components of the SC bank, $\boldsymbol{n_{sc}}$, is

$$n_{sc} = floor(U_{BUS}/U_{SCN}). \tag{9}$$

Therefore, the maximum and minimum values of the internal voltage that are considered in the sizing process are given by

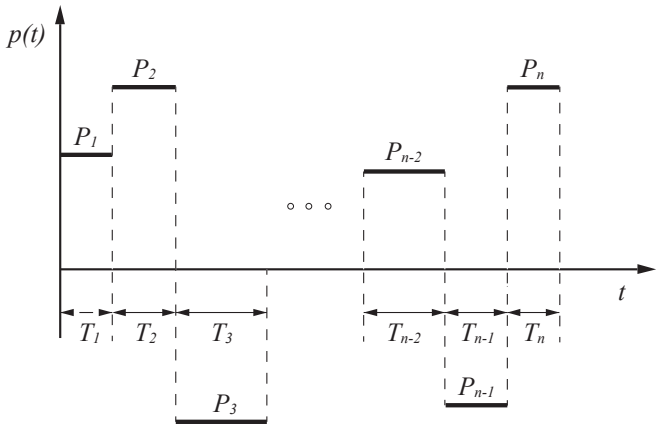

Fig. 3. Example of a SC bank power profile.

$$U_{MAX} = n_{sc} \cdot U_{SCN}, \tag{10}$$

$$U_{MIN} = 0.5 \cdot n_{sc} \cdot U_{SCN}. \tag{11}$$

The stand-by value of the internal voltage U_0, is set by the DC/DC converter and must be calculated by the proposed algorithm because of its dependence on the power profile. The new value of the internal voltage, once the time step corresponding to P_i (see Fig. 3) is completed, is U_i (see Fig. 4). Therefore, there exist $n+1$ internal voltage values within the profile to be determined. In order to avoid oversizing, two of them, U_h and U_k, should be forced to be the maximum and minimum voltage values, as seen in Fig. 4.

Equation (8) can be applied to each time interval for both the charging and the discharging processes,

$$\frac{C}{4 \cdot P_i} \cdot \left[U_I^2 - U_{i-1}^2 + U_i \cdot \sqrt{U_i^2 + 4 \cdot P_i \cdot R} - U_{i-1} \cdot \sqrt{U_{i-1}^2 + 4 \cdot P_i \cdot R} - 4 \cdot P_i \cdot R \cdot ln\left(\frac{U_{i-1} + \sqrt{U_{i-1}^2 + 4 \cdot P_i \cdot R}}{U_i + \sqrt{U_i^2 + 4 \cdot P_i \cdot R}} \right) \right] - T_i = 0 i = 1, \ldots, n., \tag{12}$$

Equation (12) represents an n-equation and (n+2)-unknown system to be solved for different values of R and whose unknowns are the $n+1$ internal voltages in Fig. 4 and the capacitance, i.e.

$$\begin{cases} f_1(U_0, \ldots, U_n, C) = 0 \\ \vdots \\ f_i(U_0, \ldots, U_n, C) = 0 \\ \vdots \\ f_n(U_0, \ldots, U_n, C) = 0. \end{cases} \tag{13}$$

The two additional equations needed to solve the system in (13) are obtained by forcing two of the internal voltages, corresponding to undetermined indexes h and k, to be the limit values,

$$U_h = U_{MAX}, \tag{14}$$

$$U_k = U_{MIN} \tag{15}$$

Values of the capacitance pertaining to the RC limit curve can be

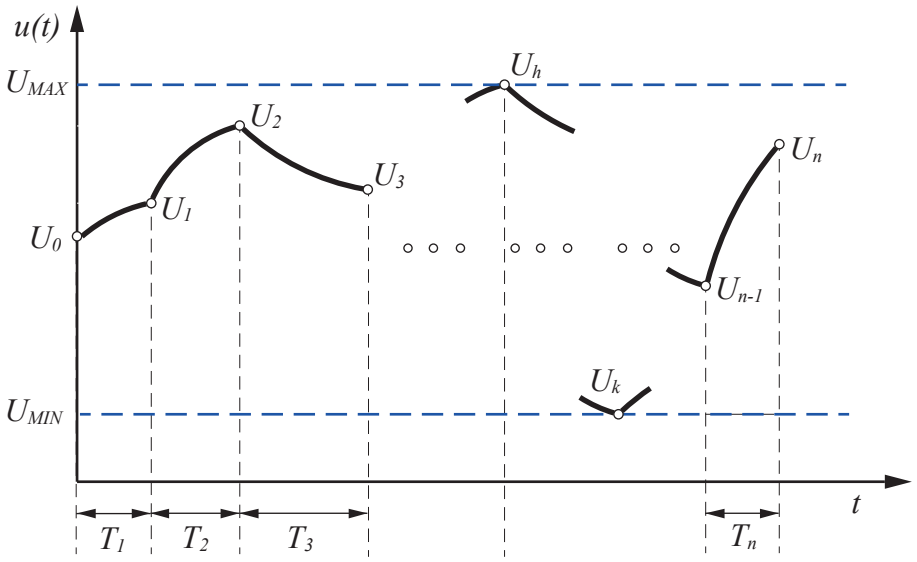

Fig. 4. Internal voltage of the SC bank.

obtained by solving the system in (13)–(15) for different values of resistance, R, within the range $0 - R_{max}$. R_{max} is the maximum internal resistance that the SC bank can have to ensure that it is capable of supplying the maximum discharge power. Notice that this limit does not apply during the charging process. According to the Maximum Power Transfer theorem, in order to guarantee the maximum discharge power, P_{max}, even with the minimum internal voltage, U_{min}, the internal resistance of the SC bank cannot exceed the value R_{max}. This threshold can be calculated as

$$R_{max} = \frac{U_{min}^2}{4 \cdot P_{max}} \tag{16}$$

P_{max} being the absolute value of the maximum discharge power,

$$P_{max} = abs(min[P_1, P_2 \ldots, P_n]) \tag{17}$$

Note that, according to the references assumed in this work, negative values P stand for discharging powers. Thus, the absolute value of the minimum of the sequence P_i provides the maximum value of the discharging power, P_{max}. Fig. 5 shows the RC limit curve which splits the RC-plane into two areas, limiting the range of acceptable solutions.

In a SC bank whose RC-pair belongs to the acceptable area (see example in Fig. 5, Ra and Ca), the internal voltage is within the range imposed by the maximum and minimum limit values. The minimum valid capacitance for the resistance in the example is given by C_{lim}. Capacitance values lower than C_{lim} lead to internal voltages in the cells beyond the acceptable limits. Therefore, once the limit curve is obtained, it is simple to assess the validity of cell combinations from the point of view of the internal voltage values. Then, the maximum current in the cells must be assessed to assure that it complies with the limit recommended by the manufacturer.

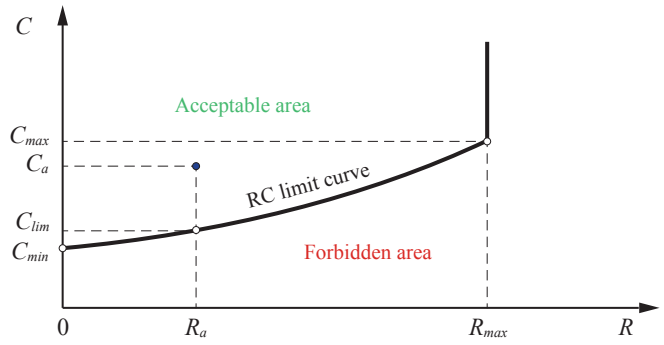

Fig. 5. RC limit curve.

The Newton-Raphson method can be efficiently used to solve the system in (13)–(15). Let $[X]^T$ be the transpose of the column vector, $[X]$, containing the unknowns, i.e, $[X] = [U_0, \ldots, U_n, C]$. The values of $[X]$ can be obtained iteratively from

$$[X]_{j+1} = [X]_j - [J]_j^{-1} \cdot [F]_j \tag{18}$$

where $[J]$ is the Jacobian matrix and $[F]$ is a column vector whose elements are the n functions in (13) particularized for iteration j,

$$f_{i(j)}\left(U_{0(j)}, \ldots, U_{n(j)}, C_{(j)}\right) \tag{19}$$

To determine the starting solution of the iterative method, a vector, $[W_{(0)}]$, containing the energy initially stored by the cells at the end of each time interval, $W_{i(0)}$, is obtained, $[W_{(0)}] = [W_{1(0)}, W_{2(0)}, \ldots, W_{n(0)}]$, where

$$W_{i(0)} = \sum_{m=1}^{i} P_m \cdot T_m, \quad i = 1, \ldots, n \tag{20}$$

If losses are assumed to be negligible, the energy balance for time interval i yields

$$\frac{1}{2} \cdot C_{(0)} \cdot \left(U_{i-1(0)}^2 - U_{i(0)}^2\right) = -P_i \cdot T_i \tag{21}$$

Since there exist n values of P_i and $n+2$ unknowns ($n+1$ voltages and the capacitance), the following system, with $n-1$ equations and without the capacitance, can be obtained by dividing each equation over the subsequent one,

$$U_{i-1(0)}^2 - \left[1 + \frac{P_i \cdot T_i}{P_{i+1} \cdot T_{i+1}}\right] \cdot U_{i(0)}^2 + \left(\frac{P_i \cdot T_i}{P_{i+1} \cdot T_{i+1}}\right) \cdot U_{i+1(0)}^2 = 0 \; i = 1, \ldots, n-1 \tag{22}$$

From vector $[W_{(0)}]$, indexes h and k, corresponding to the maximum and minimum voltages, are obtained, the two required additional equations thus being rendered,

$$W_{h(0)} = max\left(W_{1(0)}, \ldots, W_{n(0)}\right) \rightarrow U_{h(0)} = U_{MAX}, \tag{23}$$

$$W_{k(0)} = min\left(W_{1(0)}, \ldots, W_{n(0)}\right) \rightarrow U_{k(0)} = U_{MIN}. \tag{24}$$

Once the $n+1$ voltages are obtained, the initial value of the capacitance can be calculated from (21) by utilizing any of the intervals,

$$C_{(0)} = \frac{-2 \cdot P_i \cdot T_i}{\left(U_{i-1(0)}^2 - U_{i(0)}^2\right)} \tag{25}$$

Once the initial values of all the variables are known, the iterative process can be started. The Jacobian matrix can be expressed as the combination of three matrices,

$$[J] = \begin{bmatrix} [J_1][J_2] \\ [J_3] \end{bmatrix}$$

Submatrix $[J_1]$ has n rows and $n+1$ columns and is obtained by deriving each function f_i with respect to voltages U_{i-1} and U_i at iteration j,

$$\frac{\partial f_i}{\partial U_{i-1(j)}} = -\frac{C_{(j)}}{2 \cdot P_i} \cdot \left(U_{i-1(j)} + \sqrt{U_{i-1(j)}^2 + 4 \cdot R \cdot P_i}\right) \tag{26}$$

$$\frac{\partial f_i}{\partial U_{i(j)}} = \frac{C_{(j)}}{2 \cdot P_i} \cdot \left(U_{i(j)} + \sqrt{U_{i(j)}^2 + 4 \cdot R \cdot P_i}\right), i = 1, \ldots, n \tag{27}$$

Submatrix $[J_2]$ is a column vector with n rows that are obtained by deriving functions f_i with respect to the capacitance,

$$\frac{1}{4 \cdot P_i} \cdot \left[U_i^2 - U_{i-1}^2 + U_i \cdot \sqrt{U_i^2 + 4 \cdot P_i \cdot R} - U_{i-1} \cdot \sqrt{U_{i-1}^2 + 4 \cdot P_i \cdot R} - 4 \cdot P_i \cdot R \cdot Ln\left(\frac{U_{i-1} + \sqrt{U_{i-1}^2 + 4 \cdot P_i \cdot R}}{U_i + \sqrt{U_i^2 + 4 \cdot P_i \cdot R}}\right)\right] \tag{28}$$

Submatrix $[J_3]$ has two rows and $n+2$ columns, and corresponds to the derivative of equations 23 and 24 with respect to voltages U_h and U_k,

$$[J_3] = \begin{bmatrix} 0 & 0 & \ldots & 0 & \overbrace{1}^{\text{Index h}} & 0 & \ldots & 0 & 0 \\ 0 & 0 & \ldots & 0 & \ldots & 0 & \underbrace{1}_{\text{Index k}} & \ldots & 0 \end{bmatrix} \tag{29}$$

The indexes h and k can vary from one iteration to another. There may be a change in the step of considering the calculation of U_i without taking into account the resistances with respect to the case of considering them but, once losses are included in iterations, those indices will be the same. Once a set of points in the RC limit curve is obtained by solving the system for various values of R between 0 and R_{max}, the curve can be adjusted by using the method of least squares to a polynomic function,

$$C = a_0 + a_1 \cdot R + \ldots + a_m \cdot R^m \quad \forall R \varepsilon (0, R_{max}) \tag{30}$$

A polynomial with a degree of 2 or 3 results in an accurate adjustment for this application and avoids overfitting issues which may arise with higher orders. The value of the coefficient a_0 corresponds to an ideal capacitance, i.e. the capacitance of a lossless SC ($R = 0$), that complies with the voltage and power constraints. Any real design must include a higher capacitance value that the one imposed by this threshold. A pre-condition to select a feasible design is to assure that the combination of cells leads to an equivalent capacitance of the SC bank higher than the ideal one. Once the number and connection of those cells are obtained, their equivalent resistance is calculated. Then, it must be verified that the RC pair is above the limit curve. Otherwise, the number of parallel-connected cells of each series-connected element can be increased both to decrease the series resistance and to increase the capacitance.

Fig. 6 shows the flowchart of the algorithm, where n_p stands for the number of points utilized to create the RC limit curve. The value of n_p can be arbitrarily chosen by the designer. A higher value of n_p increases the accuracy of the curve resulting from the fitting process. However, a lower value of n_p can be used to boost the execution time of the design algorithm. Input data are the power and time interval vectors, the dc-bus voltage, the rated voltage of the capacitance of the selected cells and the number of points of the RC limit curve, n_p. The values ε_1 and ε_2 are thresholds used to stop the iterative process in the calculation of internal voltages and capacity, respectively, and can be defined by the user.

5. Case study

In this section, a case study is presented in order to illustrate the utility and effectiveness of the described method. The sizing of a SC bank, intended to compensate the power oscillations of an adjustable speed drive (ASD) guiding an industrial lift, is tackled here below. A record of the active power absorbed by this facility, was taken during 17 min with a time step of 3 s. Thus, the charging power vector used as an input to the algorithm includes a total number, n, of 340 elements. The resulting power profile is shown in Fig. 7, which allows confirming that the dynamics of the process has effectively been captured.

The key values of the power profile are highlighted in Table I. If the SCs bank is in charge of the oscillations in the power of system B, $p_B(t)$, the main source must generate a constant power equal to the mean value of $p_B(t)$, $\overline{p_B}$, which is 5.25 kW in this case. However, should the SCs bank were not installed, the main source must supply up to 28.85 kW, which provokes higher losses and voltage drops in the network. Moreover, such high power fluctuations increase the network harmonic contents, which can trigger protections, increase transformer and motor losses, etc.

From the aforementioned record, the power profile to be used in the design of a SC solution with load leveling purposes, which is shown in Fig. 8, can be easily obtained. The SC set is connected directly to the 540 V DC bus of the ASD through a DC-DC bidirectional converter. Thus, according to (2), the power demanded by the SC set, $p(t)$, follows the oscillations of the load excluding its mean power, which, on the other hand, is efficiently provided by the grid on an constant basis.

In the design of the present solution, the SC cells offered by Maxwell Technologies have been considered [31,32]. These cells

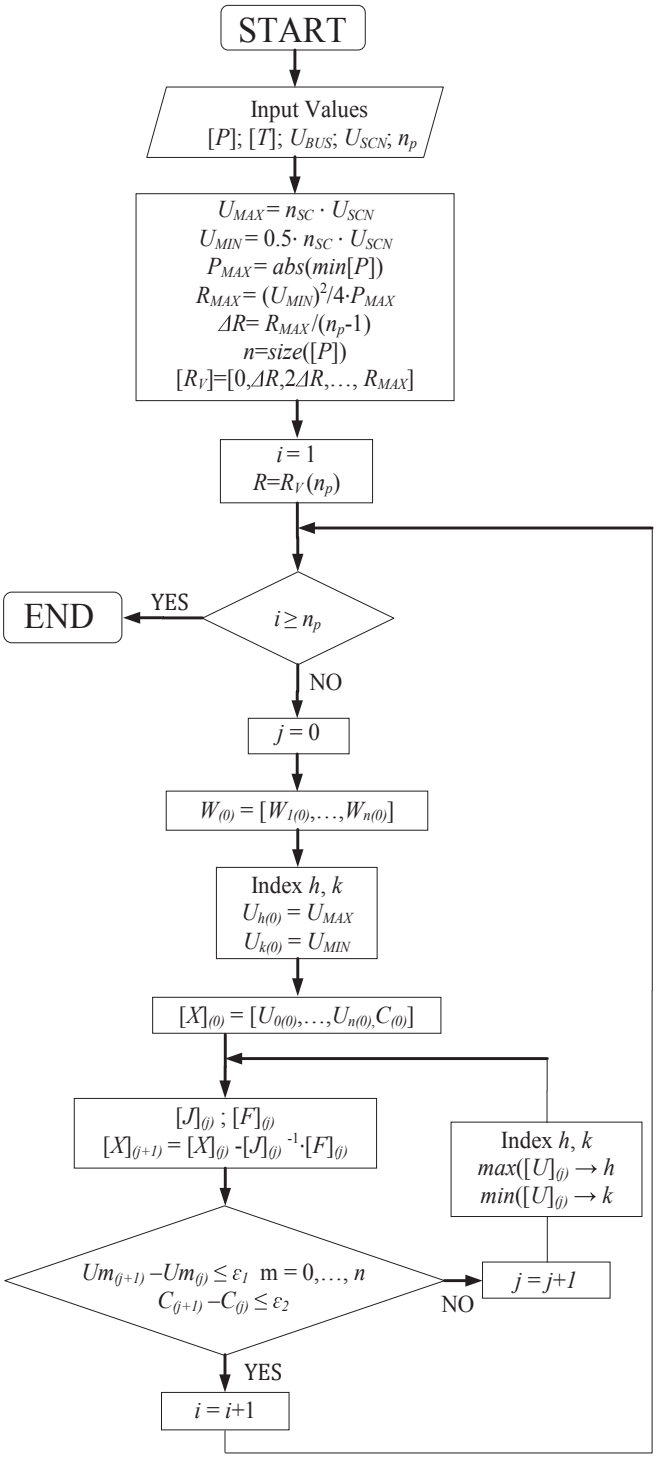

Fig. 6. Algorithm flowchart.

have a rated voltage of 2.7 V. Thus, 200 individual cells or shunt associations of cells are connected in series leading to a maximum voltage of 540 V and a minimum voltage of 270 V (in order to comply with the lowest voltage limit recommendations of the manufacturer, i.e. 50% of the rated value).

According to Fig. 8, the maximum discharge power to be supplied by the SC set is 23.6 kW. Thus, considering (16), the maximum acceptable value for the internal resistance of the set, R_{max}, results in 772.25 mΩ. Taking these data as a basis and applying the

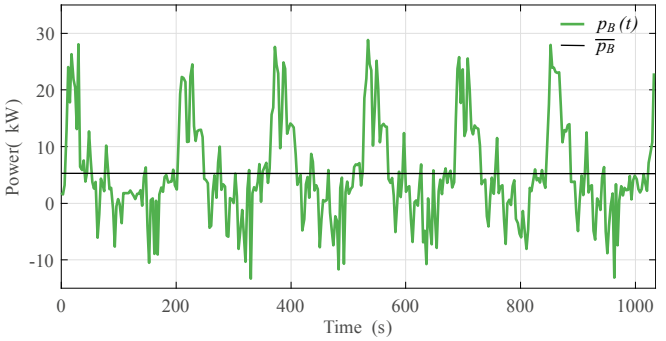

Fig. 7. Power profile of an industrial lift driven by an ASD, $p_B(t)$. The mean value is $\overline{p_B} = 5.25kW = p_A(t)$.

Table 1
KEY VALUES OF THE POWER PROFILE OF THE LOAD.

	Maximum	Minimum	Mean
Power (kW)	28.85	−13.31	5.25

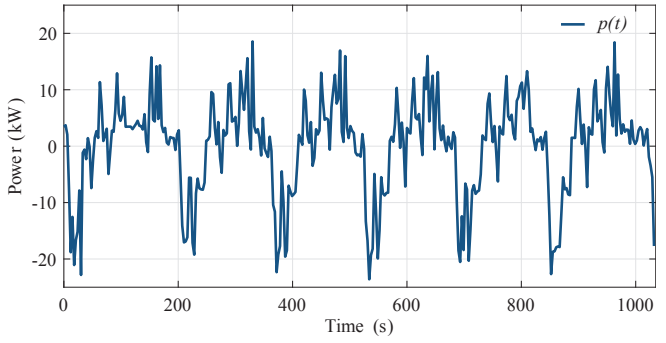

Fig. 8. Power demand profile used for the design of a SC set with load leveling purposes, $p(t) = \overline{p_B} - p_B(t)$.

algorithm described in Section IV, the internal-resistance/capacitance (RC) curve, which delimitates the range of acceptable solutions, is obtained. Before conducting the curve fitting process a number of discrete solutions, n_p, equal to 20 are obtained. This implies solving the problem for 20 resistance values using a step of $\Delta R = 40.52m\Omega$. As can be seen in Fig. 9, together with the constraint imposed by R_{max}, those points are capable of characterizing the RC limit curve in a proper way.

Using curve fitting, the RC curve can be approximated by polynomial equations. Table II shows the parameters of a first degree and second degree polynomial approximation, together with the determination coefficient, R^2. According to the latter values, both possibilities are acceptable for the present case.

Once the RC curve is available either in a graphical or mathematical formulation, stating if a specific RC pair complies with the requirements is straightforward. Furthermore, with the proposed method the effect of the resistance of connections and wiring can be easily considered in the design stage. The RC limit curve to use is the same, since it only takes into account the generic values of the resistance and capacity of the set. This also allows to verify very easily if a certain combination of cells is valid at different temperatures. Since both R and C vary with temperature, and this variation is provided by the manufacturer, then it is possible to know if the chosen RC pair is valid or not. It can happen that a combination whose RC pair is in the acceptable area at 20 °C, and yet go to the

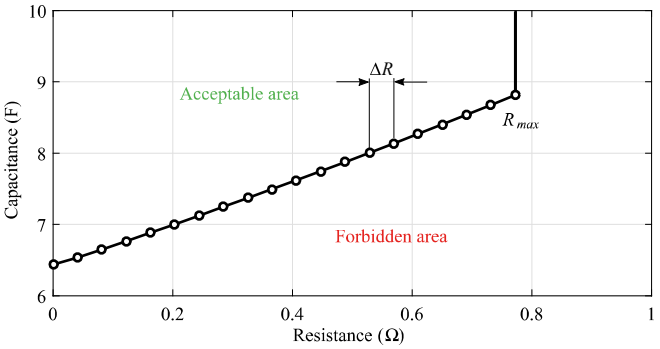

Fig. 9. RC curve. Acceptable and forbidden areas for the range of solutions.

Table 2
Curve Fitting parameters and correlation coefficients.

Poly. degree	Fitting parameters			R^2
	a_0	a_1	a_2	
First	6.3859	3.0934	–	0.9991
Second	6.4282	2.7464	0.4493	0.9999

forbidden area at −30 °C, due to the increase in internal resistance.

For the present case study, the ideal capacitance of the SC set at the end of its useful life is 6.4282 F (i.e. one with a negligible internal resistance). Therefore, each of the series connected elements should provide 1285.64 F in this ideal case. For a better comprehension of the phenomenon, Fig. 10 shows the internal voltage profile for three different cases located over the RC curve. The specific values used in those simulations are highlighted in Table III, and correspond to the ideal case, i.e. $R_{eq} = 0$, $C_{LIM}1$, a case with an internal resistance close to the stability limit, $C_{LIM}3$, and an intermediate value, $C_{LIM}2$.

In order to obtain the curves shown in Fig. 10, the procedure shown in Fig. 6 has been used. In the present case, R and C are already known for each particular combination under analysis. The internal voltage at the end of each sample, together with the initial internal voltage (i.e. the stand-by voltage U_0), are obtained from the system of equations described in Section IV. However, a degree of freedom already exists in this case, as there are $n+1$ unknowns and only n equations. To turn this undetermined system of equations on a fully determined one, a sensible choice is to impose that the resulting curve remains centered, at each iteration, j, within the acceptable range, i.e.

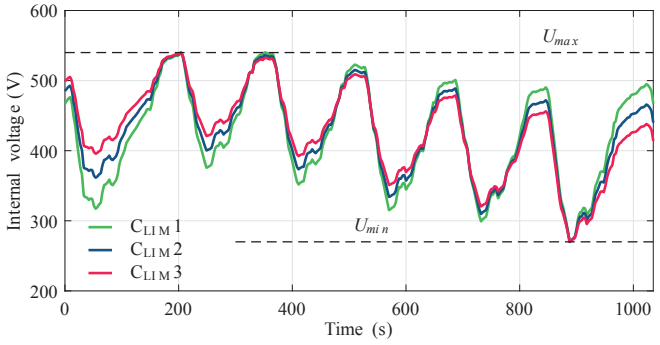

Fig. 10. Internal voltage for three borderline combinations. $C_{LIM}1$: ideal case, $C_{LIM}2$: intermediate resistance value, and $C_{LIM}3$: resistance value close to the stability limit.

Table 3
Set of combinations over the RC curve.

Case	SC bank	
	R_{eq} (Ω)	C_{eq}(F)
$C_{LIM}1$	0	6.428
$C_{LIM}2$	0.3658	7.495
$C_{LIM}3$	0.7723	8.818

$$U_h(j) + U_k(j) = U_{MIN} + U_{MAX}. \quad (31)$$

For this set of borderline combinations, the maximum and minimum internal voltage values are exactly met, but never exceeded. Specifically, the minimum internal voltage is reached at 888 s for the three cases, while the maximum value is reached at 351 s for $C_{LIM}1$ and at 204 s for $C_{LIM}2$ and $C_{LIM}3$. As can be seen in Fig. 10, each combination has a stand-by voltage, U_0, different. If each curve had started with another value of the initial voltage, some internal voltages would go beyond the limits.

Most of the manufacturers provide values of the capacitance and internal resistance of their SC cells at the start of their useful life, C_N, R_N. Thus, in order to guarantee a proper performance of the solution during its entire lifetime, an estimation of those parameters at the end of this period, C_{EOL}, R_{EOL} becomes mandatory. For the case under study, the capacitance is expected to suffer a reduction of 20% while the internal resistance an increase of 100%, according to the manufacturer Maxwell Technologies, [31,32]. These figures can be slightly different for the cells of other manufacturers, so their particular specifications should be followed in this calculation. Table IV shows the specific values of capacitance and internal resistance for a set of SC cells by Maxwell Technologies ranging from 25 F to 2000 F, given at 25 °C.

From the data shown in Table IV, some of the possible combinations of cells that may be used in the design of a SC solution for the application under study can be easily analyzed. Only the parameters estimated for the end of life of the cells are considered in the analysis. If the requirements are met in this extreme condition, a proper performance is assured for the entire lifetime. Obviously, all the combinations selected for this study shows a capacitance higher than the one calculated for the ideal case, i.e. 6.4282 F. A lower value would undoubtedly fail to meet the requirements. Table V shows six of the possible combinations, C1 to C6, which can be achieved by using the cells in Table IV. The second column in Table V states the number of cells in parallel connection used to build each of the 200 series elements used in the SC solution. Furthermore, the said column shows the rated capacitance of the selected cells.

The internal-resistance/capacitance (RC) pairs of the different combinations are displayed in Fig. 11. As it is straightforward derived from this figure, combinations C4 and C5 do not comply with the requirements, despite their capacitance is higher than the required by the ideal case. Conversely, combinations C1, C2, C3 and C6 are valid solutions, since all of them lie within the acceptable area. Notice that C3 is the one with a lower internal resistance, so this solution provides the best behavior in terms of power losses.

The internal voltage values in the time domain for cases C1, C2 and C4 are depicted in Fig. 12. To obtain them, the system given by (13) and (31), for a known RC pair, has been solved in the same way as in the previous example. For the latter case, the internal voltage of the SC bank clearly exceeds the admissible voltage limits. On the contrary, C1 and C2 are able to maintain the internal voltage value within the required acceptable range.

In cases C1 and C2, the resulting selection of the stand-by voltage leads to the highest security margin, i.e. the probability of

Table 4
SC cell values drift during their lifetime.

Start of life (SOL)		End of life (EOL)	
C_N (F)	R_N (mΩ)	C_{EOL} (F)	R_{EOL}(mΩ)
25	42	20	84
50	20	40	40
100	15	80	30
150	14	120	28
650	0.8	520	1.6
1200	0.58	960	1.16
1500	0.47	1200	0.94
2000	0.35	1600	0.7

Table 5
Cases for the analysis of the design of a SC bank.

Comb.	Serial element	Individual cell param. (EOL)		SC bank param. (EOL)	
		C_{EOL} (F)	R_{EOL}(mΩ)	C_{eq} (F)	R_{eq} (Ω)
C1	1 × 2000 F	1600	0.70	8.0	0.1400
C2	2 × 1200 F	960	1.16	9.6	0.1160
C3	3 × 650 F	520	1.60	7.8	0.1067
C4	11 × 150 F	120	28	6.6	0.5091
C5	12 × 150 F	120	28	7.2	0.4667
C6	13 × 150 F	120	28	7.8	0.4308

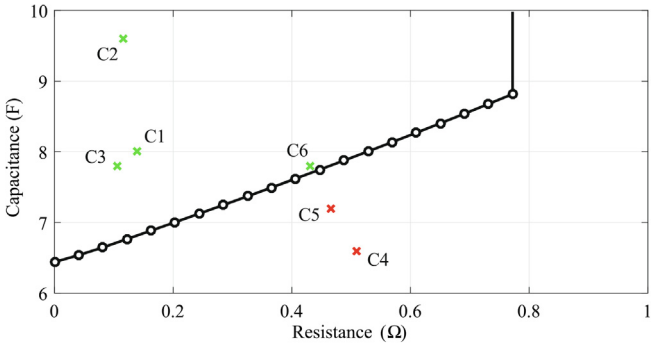

Fig. 11. RC pairs for six possible combinations of SC cells. Acceptable solutions (green), invalid solutions (red).

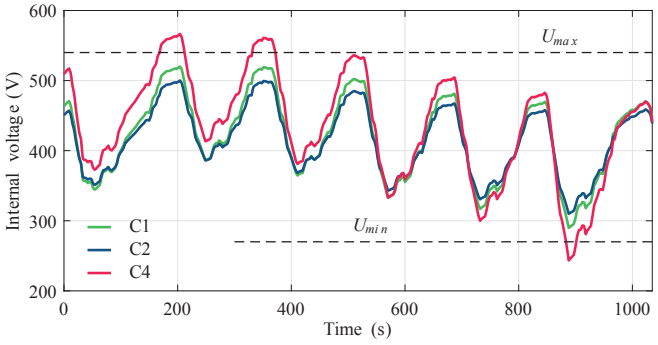

Fig. 12. Internal voltage value, $\boldsymbol{u}(\boldsymbol{t})$, for different combinations of SC cells.

remaining within the limits under a spurious excursion of the power profile is maximized.

Starting from the internal voltage, the current of the SC bank can be easily obtained from (4) and (7). In Fig. 13, the current profile for the case of a valid RC pair such as C1 is shown. The

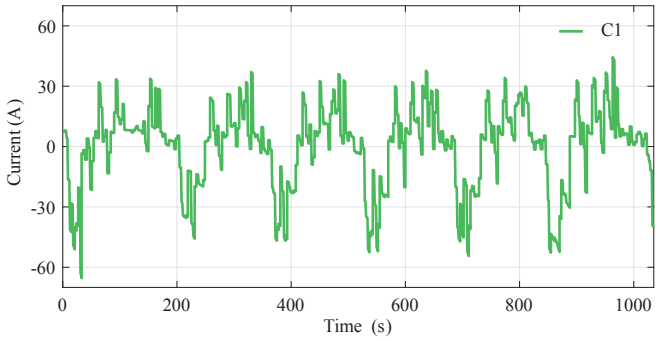

Fig. 13. Current profile for the SC bank designed according to the specifications of case C1.

absolute peak current to be handled by this combination is thus evaluated in 65.4 A.

In a discharge process, $P_i < 0$, the maximum current will be given at the end of the interval, T_i, when the internal voltage is minimum, that is

$$i_{max\_i} = \frac{-U_i}{2 \cdot R} + \frac{\sqrt{U_i^2 + 4 \cdot P_i \cdot R}}{2 \cdot R}. \tag{32}$$

On the contrary, in a charging process, $P_i > 0$, the maximum current will occur at the beginning of the interval, and it can be obtained with Ui-1, instead of Ui in (32).

In order to summarize the results for the six cases specified in Tables V, VI shows the maximum and minimum internal voltage, stand-by voltage and absolute peak current, both for the SC bank and for the individual cells. As a final verification, the designer should check that the maximum current of the selected cells does not exceed the recommendation of the manufacturer. This limit is quite far from the present values for the current case study.

The proposed method also allows a fast assessment of the energy processes derived from a particular solution. Thus, by simply applying Joule's Law, the total energy losses caused by the internal resistance of the proposed SC solution can be evaluated. Through an energy balance in each time interval, T_i, the energy dissipated in the internal resistance is easily obtained. In a charging process, $P_i > 0$, it can be written:

$$P_i \cdot T_i = \frac{1}{2} \cdot C \cdot \left(U_i^2 - U_{i-1}^2 \right) + W_{losses}. \tag{33}$$

Substituting the value of T_i given by (12), the dissipated energy is obtained according to the initial and final internal voltages,

Table 6
Main results for the different SC solutions under analysis.

Case	Min. voltageU_k (V)	Max. voltageU_h (V)	Stand-byU_0 (V)	Max. current SC bank (A)	Max. current Cell (A)	Individual cell current limit (A)
C1	289.82	520.18	463.27	65.40	65.40	1500
C2	309.94	500.00	450.68	64.30	32.15	960
C3	288.59	521.40	462.49	65.68	21.89	680
C4	243.43	566.57	509.25	64.16	5.83	65
C5	258.95	551.05	496.67	64.46	5.37	65
C6	271.75	538.24	486.56	64.54	4.96	65

$$W_{losses}=\frac{C}{4}\cdot\left[U_{i-1}^2-U_i^2+U_i\cdot\sqrt{U_i^2+4\cdot P_i\cdot R}-U_{i-1}\cdot\sqrt{U_{i-1}^2+4\cdot P_i\cdot R}-4\cdot P_i\cdot R\cdot L_n\left(\frac{U_{i-1}+\sqrt{U_{i-1}^2+4\cdot P_i\cdot R}}{U_i+\sqrt{U_i^2+4\cdot P_i\cdot R}}\right)\right] \quad (34)$$

In the discharge process, the formula is the same, changing the sign of the power. To calculate the efficiency in the charging processes, the following expression will be used

$$\eta_{ch}=\frac{\sum_{j=1}^{n}0.5\cdot C\cdot\left(U_j^2-U_{j-1}^2\right)}{\sum_{j=1}^{n}P_j\cdot T_j},\ P_j>0. \quad (35)$$

In the discharge processes, the efficiency is given by

$$\eta_{dch}=\frac{\sum_{k=1}^{m}|P_k|\cdot T_k}{\sum_{k=1}^{m}0.5\cdot C\cdot\left(U_k^2-U_{k-1}^2\right)},\ P_j<0 \quad (36)$$

Finally, the mean dissipated power of each combination can be easily calculated with the following expression

$$P_{losses\_mean}=\frac{\sum_{i=1}^{n}W_{losses\_i}}{\sum_{i=1}^{n}T_i}, \quad (37)$$

where the term W_{losses_i} is given by equation (34) for each time, Ti. All this values are shown in Table VII. Only those combinations which comply with the constraints of the particular application of the present case study are displayed in the said table. Thus, case C3 results in the combination with the lowest power losses. This design is built with series elements formed by 3 cells connected in parallel, each with a rated capacitance of 650 F. On the opposite side, case C6, which is built with series elements made up from the parallel combination of 13 cells of 150 F results in the solution with the lowest efficiency.

The proposed method gives all the necessary tools to take the final design decision, which can be finally selected considering financial concerns (including both the annualized investment and operational costs from power losses), or even reliability issues (number of elements in the final set).

6. Advantages of the proposed method

The advantages of the proposed method are summarized as follows:

1) The method solves the most general case in a simple way, i.e. when the SC or SCs bank is subjected to a succession of positive or negative constant power values of any duration. Therefore, any particular case can be solved with the proposed method just by modifying the number of values in *P*, their signs or the duration of the corresponding time intervals.

2) The method does not provide just one particular solution; conversely, the method demarcates the area in the RC plane where the infinite possible solutions fall within, which allows the designer greater freedom of choice when selecting an RC pair to meet the system requirements.
3) The method does not restrict elements in series to be considered as just one single cell. Most authors in the bibliography resort to seeking for RC pairs within those provided by manufacturers of a specific SC series. In the proposed method, the RC limit curve depends only on the power profile and the mínimum and maximum internal voltages. Therefore, once the RC limit curve has been obtained, different RC pairs from diverse manufacturers can be assessed.
4) The method allows the evaluation of the RC pair selected at different temperatures from the data provided by the manufacturer.
5) The method enables the assessment of the effect of the increase in R due to the resistance of cables and connections.
6) The method enables the assessment of any solutions proposed by other methods just by using the RC limit curve. For instance, in Ref. [30], a SCs bank subjected to a power profile comprising three 5-s discharge values, $P(W)=[-105,-213,-319]$, is sized.Therefore, $T(s)=[5,5,5]$. The method in Ref. [30] starts from $V_{max}=16.65$ V and the internal voltage is forced not to get below $V_{min}=10$ V. The solution proposed in Ref. [30] is a SC whose parameters are R = 0.059 Ω and C = 52.6 F. If the RC limit curve is calculated under these circumstances, the result can be assimilated to a 3rd-order polynomial, $C=5877{,}3\,R^3-145{,}39\,R^2+62{,}075R+35{,}926$. For R = 0.059 Ω, the capacitance at the RC limit curve is 40.289 F; therefore, for C = 52.6 F, the RC pair falls within the acceptable area and, as said in Ref. [30], the solution is slightly oversized.

Table 7
Losses for the different SC solutions under analysis.

Case	Dissipated energy (kJ)	Av. power losses (W)	Efficiency on charge (%)	Efficiency on discharge (%)
C1	60.3	58.2	99.32	98.86
C2	50.6	48.9	99.43	99.04
C3	45.8	44.2	99.48	99.14
C6	185.6	179.3	98.02	96.48

7) The method enables the calculation of the stand-by voltage, which is the target of the so-called peak saving application. In this application, the value of the stand-by voltage needed for the SCs to face the power profile while complying with the limits is calculated along with the RC pair. Apart from considering the total charged or discharged energy at the SCs, the order in which those charge and discharge processes occur is crucial. For instance, if all the charge processes occur first, $U_0 =$ Umin. Conversely, if all the discharge processes occur first, $U_0 =$ Umax. Finally, if the charge and discharge processes alternate with each other, $U_{min} < U_0 < U_{max}$.

7. Conclusions

In this contribution, a new method for the correct sizing of SC banks is proposed. A general case is taken as a basis, in which the power profile is known in advance. This is a common case in popular SC applications such as those devoted to load leveling or peak shaving, in which a simple measurement campaign can provide the required data. The procedure shown is not limited to giving only one of the infinite possible solutions, as it can be found in the literature, but it allows to calculate an internal-resistance/capacitance curve which separates the acceptable set of solutions from those which are not able to comply with the requirements. From this RC curve, it is straightforward to check if a specific combination of real SC cells is suitable for the application of interest. The proposed method is not restricted to the use of single cells in series combination but to any shunt association. Thus, the losses from different commercial alternatives can be assessed and a selection based in financial concerns may be conducted. This possibility is particularly interesting for high power applications, in which high capacitance and low internal-resistance series elements are required. In this case, it is unlikely to succeed in meeting the needs with the individual elements offered by the marketers; therefore the use of cells in parallel connection may become mandatory. In addition, the algorithm allows easily the designer to check the current values in each section, in order to ensure that the recommendation of the manufacturer is not exceeded. Furthermore, with the proposed method the effect of the resistance of connections and wiring can be easily considered in the design stage, and it is also easy to verify if the chosen combination of cells is valid at different temperatures.

Declaration of interests

☒ The authors declare that they have no known competing financial interests or personal relationships that could have appeared to influence the work reported in this paper.

☐ The authors declare the following financial interests/personal relationships which may be considered as potential competing interests:

Acknowledgments

This work has been funded by the Spanish Government, Innovation Development and Research Office (MEC), under research grants ENE2014-52272-R, DPI2017-83804-R, and DPI2017-89186-R.

References

[1] Miller J. Introduction to electrochemical capacitor technology. IEEE Electr Insul Mag Jul. 2010;26(4):40–7.
[2] Kagiri C, Xia X. Optimal control of a hybrid battery/supercapacitor storage for neighborhood electric vehicles. Energy Proc May 2017;105:2145–50.
[3] Kuperman A, Aharon I. Battery-ultracapacitor hybrids for pulsed current loads: a review. Renew Sustain Energy Rev Feb. 2011;15(2):981–92.
[4] Ghenaatian HR, Mousavi MF, Rahmanifar MS. High performance battery-supercapacitor hybrid energy storage system based on self-doped polyaniline nanofibers. Synth Met Sep. 2011;161(17–18):2017–23.
[5] Jing W, Lai CH, Wong SHW, Wong MLD. Battery-supercapacitor hybrid energy storage system in standalone DC microgrids: a review. IET Renew Power Gener 2017;11(4). 461-169.
[6] Kim Y, Raghunathan V, Raghunathan A. Design and management of battery-supercapacitor hybrid electrical energy storage systems for regulation services. IEEE Trans Multi-Scale Comput Syst Jan.-Mar. 2017;3(1):12–24.
[7] Lemofouet S, Rufer A. A hybrid energy storage system based on compressed air and supercapacitors with maximum efficiency point tracking (MEPT). IEEE Trans Ind Electron Aug. 2016;53(4):1105–15.
[8] Luta DN, Raji AK. Optimal sizing of hybrid fuel cell-supercapacitor storage system for off-grid renewable applications. Energy Jan. 2019;166(1):530–40.
[9] Kouchachvili L, Yaïci W, Entchev E. Hybrid battery/supercapacitor energy storage system for the electric vehicles. J Power Sources Jan. 2018;374(15):237–48.
[10] Song Z, Hou J, Hofmann H, Li J, Ouyang M. Sliding-mode and Lyapunov function-based control for battery/supercapacitor hybrid energy storage system used in electric vehicles. Energy Mar. 2017;122(1):601–17.
[11] Yu H, Tarsitano D, Hu X, Cheli F. Real time energy management strategy for a fast charging electric urban bus powered by hybrid energy storage system. Energy Oct. 2016;112(1):322–31.
[12] Wang H, Huang Y, Khajepour A, He H, Cao D. A novel energy management for hybrid off-road vehicles without future driving cycles as *a priori*. Energy Aug. 2017;133(15):929–40.
[13] Somayajula D, Crow ML. An integrated dynamic voltage restorer-ultracapacitor design for improving power quality of the distribution grid. IEEE Trans. Sustain. Energy Apr. 2015;6(2):616–24.
[14] Grbovic PJ. Ultra-capacitors in power conversion systems. IEEE Press Wiley; 2013, ISBN 9781118356265.
[15] de la Torre S, Sánchez-Racero AJ, Aguado JA, Reyes M, Martínez O. Optimal sizing of energy storage for regenerative braking in electric railway systems. IEEE Trans Power Syst May 2015;30(3):1492–500.
[16] Parise G, Parise L, Malerba A, Pepe FM, Honorati A, Chavdarian PB. Comprehensive peak-shaving solutions for port cranes. IEEE Trans Ind Appl May/June 2017;53(3):1799–806.
[17] Musolino V, Piegari L, Tironi E. New full-frequency-range supercapacitor model with easy identification procedure. IEEE Trans Ind Electron Jan. 2013;60(1):112–20.
[18] Bertrand N, Sabatier J, Briat O, Vinassa J. Embedded fractional nonlinear supercapacitor model and its parametric estimation method. IEEE Trans Ind Electron Dec. 2010;57(12):3991–4000.
[19] J. M. Miller, Ultracapacitor applications, IET Power and Energy Series 59, 2011. ISBN: 9781849190718.
[20] Deshpande RP. Ultracapacitors. Mc Graw Hill; 2014, ISBN 9780071841672.
[21] Grbovic PJ, Delarue P, Le Moigne P, Bartholomeus P. The ultracapacitor-based regenerative controlled electric drives with power-smoothing capability. IEEE Trans Ind Electron Dec. 2012;59(12):4511–22.
[22] Thounthong P, Raël S, Davat B. Analysis of supercapacitor as second source based on fuel cell power generation. IEEE Trans Energy Convers Mar. 2009;24(1):247–55.
[23] Gyawali N, Ohsawa Y. Integrating fuel/electrolyzer/ultracapacitor system into a stand-alone microhydro plant. IEEE Trans Energy Convers Dec. 2010;25(4):1092–101.
[24] Mellincovsky M, Kuperman A, Lerman C, Gadelovits S, Aharon I, Reichbach N, Geula G, Nakash R. Performance and limitations of a constant power-fed supercapacitor. IEEE Trans Energy Convers June 2014;29(2):445–52.
[25] Zhang L, Hu X, Wang Z, Sun F, Deng J, Dorrell DG. Multiobjective optimal sizing of hybrid energy storage system for electric vehicles. IEEE Trans Veh Technol Feb. 2018;67(2):1027–35.
[26] Zhao C, Yin H, Yang Z, Ma C. Equivalent series resistance-based energy loss analysis of a battery semiactive hybrid energy storage system. IEEE Trans Energy Convers Sep. 2015;30(3).
[27] Spyker RL, Nelms RM. Classical equivalent circuit parameters for a double-layer capacitor. IEEE Trans Aerosp Electron Syst Jul. 2000;36(3):829–36.
[28] Abdel-baqi O, Nasiri A, Miller P. Dynamic performance improvement and peak power limiting using ultracapacitor storage system for hidraulic mining shovels. IEEE IEEE Trans. Ind. Electron. May 2015;62(5):3173–81.
[29] Rotenberg D, Vahidi A, Kolmanovsky I. Ultracapacitor assisted powertrains: modeling, control, sizing and the impact on fuel economy. IEEE Trans Control Syst Technol May 2011;19(3):576–89.
[30] Kuperman A, Mellincovsky M, Lerman C, Aharon I, Reichbach N, Geula G, Ronen Nakash. Supercapacitor sizing based on desired power and energy performance. IEEE Trans Power Electron Oct. 2014;29(10).
[31] Maxwell Technologies. Datasheet – HC series ultracapacitors. Document #1013793.5.
[32] Maxwell Technologies. Datasheet – K2 series ultracapacitors. Document #1015370.4.